Measurement of the associated $\gamma+\mu^{\pm}$ production cross section in $p\bar{p}$ collisions at $\sqrt{s}=1.8$ TeV

F. Abe,[13] M. G. Albrow,[7] S. R. Amendolia,[22] D. Amidei,[16] J. Antos,[28] C. Anway-Wiese,[4] G. Apollinari,[26] H. Areti,[7] M. Atac,[7] P. Auchincloss,[25] F. Azfar,[21] P. Azzi,[20] N. Bacchetta,[20] W. Badgett,[16] M. W. Bailey,[18] J. Bao,[35] P. de Barbaro,[25] A. Barbaro-Galtieri,[14] V. E. Barnes,[24] B. A. Barnett,[12] P. Bartalini,[22] G. Bauer,[15] T. Baumann,[9] F. Bedeschi,[22] S. Behrends,[3] S. Belforte,[22] G. Bellettini,[22] J. Bellinger,[34] D. Benjamin,[31] J. Benlloch,[15] J. Bensinger,[3] D. Benton,[21] A. Beretvas,[7] J. P. Berge,[7] S. Bertolucci,[8] A. Bhatti,[26] K. Biery,[11] M. Binkley,[7] F. Bird,[29] D. Bisello,[20] R. E. Blair,[1] C. Blocker,[3] A. Bodek,[25] W. Bokhari,[15] V. Bolognesi,[22] D. Bortoletto,[24] C. Boswell,[12] T. Boulos,[14] G. Brandenburg,[9] C. Bromberg,[17] E. Buckley-Geer,[7] H. S. Budd,[25] K. Burkett,[16] G. Busetto,[20] A. Byon-Wagner,[7] K. L. Byrum,[1] J. Cammerata,[12] C. Campagnari,[7] M. Campbell,[16] A. Caner,[7] W. Carithers,[14] D. Carlsmith,[34] A. Castro,[20] Y. Cen,[21] F. Cervelli,[22] H. Y. Chao,[28] J. Chapman,[16] M.-T. Cheng,[28] G. Chiarelli,[22] T. Chikamatsu,[32] C. N. Chiou,[28] L. Christofek,[10] S. Cihangir,[7] A. G. Clark,[22] M. Cobal,[22] M. Contreras,[5] J. Conway,[27] J. Cooper,[7] M. Cordelli,[8] M. Couyoumtzelis,[22] D. Crane,[1] J. D. Cunningham,[3] T. Daniels,[15] F. DeJongh,[7] S. Delchamps,[7] S. Dell'Agnello,[22] M. Dell'Orso,[22] L. Demortier,[26] B. Denby,[22] M. Deninno,[2] P. F. Derwent,[16] T. Devlin,[27] M. Dickson,[25] J. R. Dittmann,[6] S. Donati,[22] R. B. Drucker,[14] A. Dunn,[16] K. Einsweiler,[14] J. E. Elias,[7] R. Ely,[14] E. Engels, Jr.,[23] S. Eno,[5] D. Errede,[10] S. Errede,[10] Q. Fan,[25] B. Farhat,[15] I. Fiori,[2] B. Flaugher,[7] G. W. Foster,[7] M. Franklin,[9] M. Frautschi,[18] J. Freeman,[7] J. Friedman,[15] H. Frisch,[5] A. Fry,[29] T. A. Fuess,[1] Y. Fukui,[13] S. Funaki,[32] G. Gagliardi,[22] S. Galeotti,[22] M. Gallinaro,[20] A. F. Garfinkel,[24] S. Geer,[7] D. W. Gerdes,[16] P. Giannetti,[22] N. Giokaris,[26] P. Giromini,[8] L. Gladney,[21] D. Glenzinski,[12] M. Gold,[18] J. Gonzalez,[21] A. Gordon,[9] A. T. Goshaw,[6] K. Goulianos,[26] H. Grassmann,[6] A. Grewal,[21] L. Groer,[27] C. Grosso-Pilcher,[5] C. Haber,[14] S. R. Hahn,[7] R. Hamilton,[9] R. Handler,[34] R. M. Hans,[35] K. Hara,[32] B. Harral,[21] R. M. Harris,[7] S. A. Hauger,[6] J. Hauser,[4] C. Hawk,[27] J. Heinrich,[21] D. Cronin-Hennessy,[6] R. Hollebeek,[21] L. Holloway,[10] A. Hölscher,[11] S. Hong,[16] G. Houk,[21] P. Hu,[23] B. T. Huffman,[23] R. Hughes,[25] P. Hurst,[9] J. Huston,[17] J. Huth,[9] M. Incagli,[22] J. Incandela,[7] H. Iso,[32] H. Jensen,[7] C. P. Jessop,[9] U. Joshi,[7] R. W. Kadel,[14] E. Kajfasz,[7,*] T. Kamon,[30] T. Kaneko,[32] D. A. Kardelis,[10] H. Kasha,[35] Y. Kato,[19] L. Keeble,[8] R. D. Kennedy,[27] R. Kephart,[7] P. Kesten,[14] D. Kestenbaum,[9] R. M. Keup,[10] H. Keutelian,[7] F. Keyvan,[4] D. H. Kim,[7] H. S. Kim,[11] S. B. Kim,[16] S. H. Kim,[32] Y. K. Kim,[14] L. Kirsch,[3] P. Koehn,[25] K. Kondo,[32] J. Konigsberg,[9] S. Kopp,[5] K. Kordas,[11] W. Koska,[7] E. Kovacs,[7,*] W. Kowald,[6] M. Krasberg,[16] J. Kroll,[7] M. Kruse,[24] S. E. Kuhlmann,[1] E. Kuns,[27] A. T. Laasanen,[24] N. Labanca,[22] S. Lammel,[4] J. I. Lamoureux,[3] T. LeCompte,[10] S. Leone,[22] J. D. Lewis,[7] P. Limon,[7] M. Lindgren,[4] T. M. Liss,[10] N. Lockyer,[21] C. Loomis,[27] O. Long,[21] M. Loreti,[20] E. H. Low,[21] J. Lu,[30] D. Lucchesi,[22] C. B. Luchini,[10] P. Lukens,[7] J. Lys,[14] P. Maas,[34] K. Maeshima,[7] A. Maghakian,[26] P. Maksimovic,[15] M. Mangano,[22] J. Mansour,[17] M. Mariotti,[20] J. P. Marriner,[7] A. Martin,[10] J. A. J. Matthews,[18] R. Mattingly,[15] P. McIntyre,[30] P. Melese,[26] A. Menzione,[22] E. Meschi,[22] G. Michail,[9] S. Mikamo,[13] M. Miller,[5] R. Miller,[17] T. Mimashi,[32] S. Miscetti,[8] M. Mishina,[13] H. Mitsushio,[32] S. Miyashita,[32] Y. Morita,[32] S. Moulding,[26] J. Mueller,[27] A. Mukherjee,[7] T. Muller,[4] P. Musgrave,[11] L. F. Nakae,[29] I. Nakano,[32] C. Nelson,[7] D. Neuberger,[4] C. Newman-Holmes,[7] L. Nodulman,[1] S. Ogawa,[32] S. H. Oh,[6] K. E. Ohl,[35] R. Oishi,[32] T. Okusawa,[19] C. Pagliarone,[22] R. Paoletti,[22] V. Papadimitriou,[31] S. P. Pappas,[35] S. Park,[7] J. Patrick,[7] G. Pauletta,[22] M. Paulini,[14] L. Pescara,[20] M. D. Peters,[14] T. J. Phillips,[6] G. Piacentino,[2] M. Pillai,[25] R. Plunkett,[7] L. Pondrom,[34] N. Produit,[14] J. Proudfoot,[1] F. Ptohos,[9] G. Punzi,[22] K. Ragan,[11] F. Rimondi,[2] L. Ristori,[22] M. Roach-Bellino,[33] W. J. Robertson,[6] T. Rodrigo,[7] J. Romano,[5] L. Rosenson,[15] W. K. Sakumoto,[25] D. Saltzberg,[5] A. Sansoni,[8] V. Scarpine,[30] A. Schindler,[14] P. Schlabach,[9] E. E. Schmidt,[7] M. P. Schmidt,[35] O. Schneider,[14] G. F. Sciacca,[22] A. Scribano,[22] S. Segler,[7] S. Seidel,[18] Y. Seiya,[32] G. Sganos,[11] A. Sgolacchia,[2] M. Shapiro,[14] N. M. Shaw,[24] Q. Shen,[24] P. F. Shepard,[23] M. Shimojima,[32] M. Shochet,[5] J. Siegrist,[29] A. Sill,[31] P. Sinervo,[11] P. Singh,[23] J. Skarha,[12] K. Sliwa,[33] D. A. Smith,[22] F. D. Snider,[12] L. Song,[7] T. Song,[16] J. Spalding,[7] L. Spiegel,[7] P. Sphicas,[15] L. Stanco,[20] J. Steele,[34] A. Stefanini,[22] K. Strahl,[11] J. Strait,[7] D. Stuart,[7] G. Sullivan,[5] K. Sumorok,[15] R. L. Swartz, Jr.,[10] T. Takahashi,[19] K. Takikawa,[32] F. Tartarelli,[22] W. Taylor,[11] P. K. Teng,[28] Y. Teramoto,[19] S. Tether,[15] D. Theriot,[7] J. Thomas,[29] T. L. Thomas,[18] R. Thun,[16] M. Timko,[33] P. Tipton,[25] A. Titov,[26] S. Tkaczyk,[7] K. Tollefson,[25] A. Tollestrup,[7] J. Tonnison,[24] J. F. de Troconiz,[9] M. Turcotte,[29] N. Turini,[22] N. Uemura,[32] F. Ukegawa,[21] G. Unal,[21] S. C. van den Brink,[23] S. Vejcik III,[16] R. Vidal,[7] M. Vondracek,[10] D. Vucinic,[15] R. G. Wagner,[1] R. L. Wagner,[7] N. Wainer,[7] R. C. Walker,[25] C. Wang,[6] C. H. Wang,[28] G. Wang,[22] J. Wang,[5] M. J. Wang,[28] Q. F. Wang,[26] A. Warburton,[11] G. Watts,[25] T. Watts,[27] R. Webb,[30] C. Wei,[6] C. Wendt,[34] H. Wenzel,[14] W. C. Wester III,[7] T. Westhusing,[10] A. B. Wicklund,[1] E. Wicklund,[7] R. Wilkinson,[21] H. H. Williams,[21] P. Wilson,[5] B. L. Winer,[25] J. Wolinski,[30] D. Y. Wu,[16] X. Wu,[22] J. Wyss,[20] A. Yagil,[7] W. Yao,[14] K. Yasuoka,[32] Y. Ye,[11] G. P. Yeh,[7] P. Yeh,[28] M. Yin,[6] J. Yoh,[7] C. Yosef,[17] T. Yoshida,[19] D. Yovanovitch,[7] I. Yu,[35] J. C. Yun,[7] A. Zanetti,[22] F. Zetti,[22] L. Zhang,[34] S. Zhang,[16] W. Zhang,[21] and S. Zucchelli[2]

(CDF Collaboration)

[1]*Argonne National Laboratory, Argonne, Illinois 60439*
[2]*Istituto Nazionale di Fisica Nucleare, University of Bologna, I-40126 Bologna, Italy*
[3]*Brandeis University, Waltham, Massachusetts 02254*

^{4}*University of California at Los Angeles, Los Angeles, California 90024*
^{5}*University of Chicago, Chicago, Illinois 60637*
^{6}*Duke University, Durham, North Carolina 27708*
^{7}*Fermi National Accelerator Laboratory, Batavia, Illinois 60510*
^{8}*Laboratori Nazionali di Frascati, Istituto Nazionale di Fisica Nucleare, I-00044 Frascati, Italy*
^{9}*Harvard University, Cambridge, Massachusetts 02138*
^{10}*University of Illinois, Urbana, Illinois 61801*
^{11}*Institute of Particle Physics, McGill University, Montreal, Canada H3A 2T8*
and University of Toronto, Toronto, Canada M5S 1A7
^{12}*The Johns Hopkins University, Baltimore, Maryland 21218*
^{13}*National Laboratory for High Energy Physics (KEK), Tsukuba, Ibaraki 305, Japan*
^{14}*Lawrence Berkeley Laboratory, Berkeley, California 94720*
^{15}*Massachusetts Institute of Technology, Cambridge, Massachusetts 02139*
^{16}*University of Michigan, Ann Arbor, Michigan 48109*
^{17}*Michigan State University, East Lansing, Michigan 48824*
^{18}*University of New Mexico, Albuquerque, New Mexico 87131*
^{19}*Osaka City University, Osaka 588, Japan*
^{20}*Universita di Padova, Istituto Nazionale di Fisica Nucleare, Sezione di Padova, I-35131 Padova, Italy*
^{21}*University of Pennsylvania, Philadelphia, Pennsylvania 19104*
^{22}*Istituto Nazionale di Fisica Nucleare, University and Scuola Normale Superiore of Pisa, I-56100 Pisa, Italy*
^{23}*University of Pittsburgh, Pittsburgh, Pennsylvania 15260*
^{24}*Purdue University, West Lafayette, Indiana 47907*
^{25}*University of Rochester, Rochester, New York 14627*
^{26}*Rockefeller University, New York, New York 10021*
^{27}*Rutgers University, Piscataway, New Jersey 08854*
^{28}*Academia Sinica, Taiwan 11529, Republic of China*
^{29}*Superconducting Super Collider Laboratory, Dallas, Texas 75237*
^{30}*Texas A&M University, College Station, Texas 77843*
^{31}*Texas Tech University, Lubbock, Texas 79409*
^{32}*University of Tsukuba, Tsukuba, Ibaraki 305, Japan*
^{33}*Tufts University, Medford, Massachusetts 02155*
^{34}*University of Wisconsin, Madison, Wisconsin 53706*
^{35}*Yale University, New Haven, Connecticut 06511*

We present the first measurement of associated direct photon+muon production in hadronic collisions, from a sample of 1.8 TeV $p\bar{p}$ collisions recorded with the Collider Detector at Fermilab. Quantum chromodynamics (QCD) predicts that these events are primarily from the Compton scattering process $cg \rightarrow c\gamma$, with the final state charm quark producing a muon. Hence this measurement is sensitive to the charm quark content of the proton. The measured cross section of 29 ± 9 pb is compared to a leading-order QCD parton shower model as well as a next-to-leading-order QCD calculation. [S0556-2821(99)07121-0]

Direct photon production in hadronic interactions has historically provided precise tests of quantum chromodynamics (QCD). The associated production of charm quarks in direct photon events provides a potential probe of the charm quark content of the proton through the Compton scattering process $cg \rightarrow c\gamma$ as shown in Fig. 1a [1]. In a previous publication [2] we tagged the charm quark with a full reconstruction of a D^* meson. In this paper we present the first measurement of the associated production cross section of $\gamma + \mu$ in hadron-hadron collisions. In addition, since the previous publication next-to-leading order QCD (NLO QCD) calculations [1] have become available. At NLO some new processes, which

produce a significant increase in the number of photon +charm quark events, enter the QCD calculations. The largest of these new processes is $gg \rightarrow c\bar{c}\gamma$, which is depicted in Fig. 1b.

The data for this analysis consists of an integrated luminosity of 13.2 pb^{-1} of $p\bar{p}$ collisions collected by the Collider Detector at Fermilab (CDF) in the 1992–1993 Tevatron collider run (run 1a). The CDF detector has been described in detail elsewhere [3]. The events in the photon data sample discussed in this paper contain a cluster of energy in the central electromagnetic calorimeter $|\eta_\gamma| < 0.9$, with no charged tracks pointing to the cluster. The clusters are required to have a transverse momentum $P_T[=P\sin(\theta)]$ between 17 and 40 GeV and to be isolated, with less than 2 GeV of additional transverse energy in a cone of ΔR
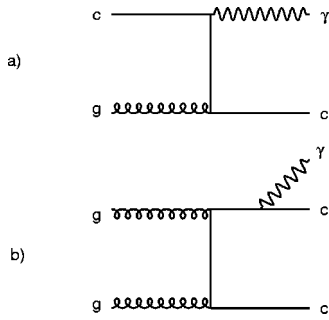
---

*Visitor.

FIG. 1. Two diagrams depicting the QCD picture of photon +charm quark production. In (a) the dominant diagram is depicted, the Compton scattering process which enters at leading order in QCD. (b) represents the largest process that enters the QCD calculation for the first time at next-to-leading order.

FIG. 2. The difference in azimuthal angle between the photon and the muon candidate is shown for the direct photon events.

$=\sqrt{\Delta \phi^2 + \Delta \eta^2}=0.7$ around the cluster. Additional photon cuts were used which were identical to those used in the run 1a CDF inclusive photon analysis [4], after these cuts 108K photon candidate events remain. Direct photon backgrounds from π^0 and η meson decays remain in the sample. They are subtracted on a statistical basis by using the photon background subtraction ''profile'' method described in Ref. [4]. The upper cut on photon P_T described above is necessary in order to use this technique. Using this method, the data sample is estimated to contain $35 \pm 7\%$ background from meson decays, leaving 70K direct photon events before muon selection.

Muon candidates in this direct photon sample were selected by additionally requiring a match between a charged track with $P_T > 4$ GeV in the central tracking chamber and a track in the appropriate muon system. For $|\eta_{\mu}| < 0.6$ the central muon system and central muon upgrade provide mostly redundant coverage and matching tracks were required in each system, while for $0.6 < |\eta_{\mu}| < 1.0$ the track was required to be in the central muon extension. All three muon systems and their respective muon identification are discussed in detail in Ref. [5], the identification is similar to that used in Ref. [6]. After the track matching requirement there are 140 ± 39 direct photon events with muon candidates (after the photon background subtraction described above). The azimuthal angular difference between the direct photon and the muon candidate is shown in Fig. 2, showing that they are very back-to-back as expected for the $2 \rightarrow 2$ scattering process.

A number of quantities that define the quality of the muon candidates, such as the position match between the track and the muon stub, were compared to a clean sample of muons from J/ψ decays, and were found to be in excellent agreement. A small background due to accidental track-stub matches was found in the central muon extension, and subtracted as discussed in Ref. [5]. No corresponding background was found in the other muon systems. Note that some of the muon candidates are muons from charged pion and kaon decays (decay-in-flight), while a smaller fraction are from charged hadrons that do not interact significantly in the material in front of the muon detectors (punch through).
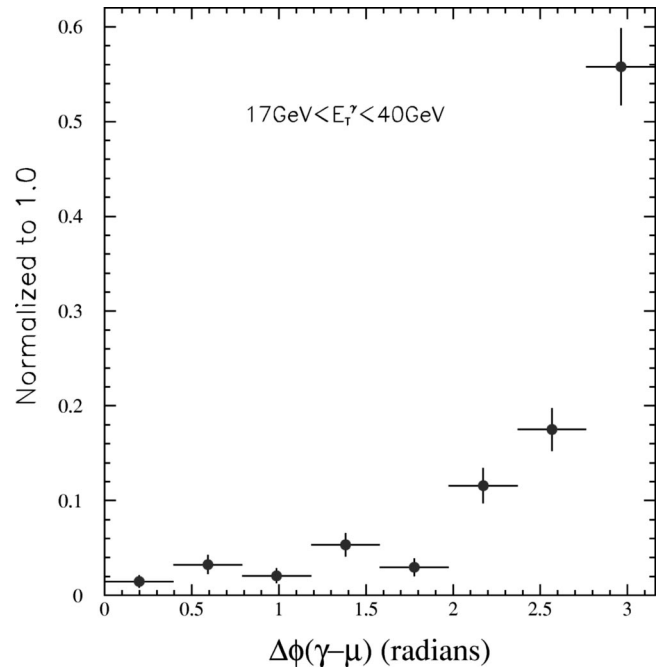
These backgrounds are estimated with a study that includes both data and Monte Carlo simulation. Starting with the parent inclusive photon+jet data sample, where the main muon backgrounds come from, we measure the 4-vector of each charged particle. These charged particles include those from the jet as well as from the underlying event in the collision. We then pass this 4-vector into a CDF detector simulation as a charged pion or kaon or proton. Finally the results of the simulation are passed through the muon reconstruction, and the number of charged hadrons that faked a muon is recorded. Approximately 75% of the background is from decay-in-flight. This background estimate should be robust since the charged particle spectrum is measured directly from the parent data sample and the kinematics of decay-in-flight are well known. The backgrounds from non-interacting protons are negligible due to their relatively large interaction cross section, thus only the particle fractions of pions and kaons need to be determined to complete the muon background estimate. A number of pion and kaon particle fraction measurements exist at the CERN e^+e^- collider LEP and the Tevatron [5], and they are quite consistent with one another. We have used the LEP measurements of 65% charged pion and 25% charged kaon as the nominal estimate since the kinematics of those measurements are best matched to the current analysis. We have used the other measurements to determine the systematic uncertainty (the largest deviation being 60% pion and 20% kaon). Combining the simulation results with the particle fractions gives the muon background rate in the direct photon sample. Figure 3 shows the muon P_T in the direct photon sample, along with the estimated muon backgrounds. One sees that the number of muon candidates is significantly larger than the estimated background. The estimated background can also be checked directly by
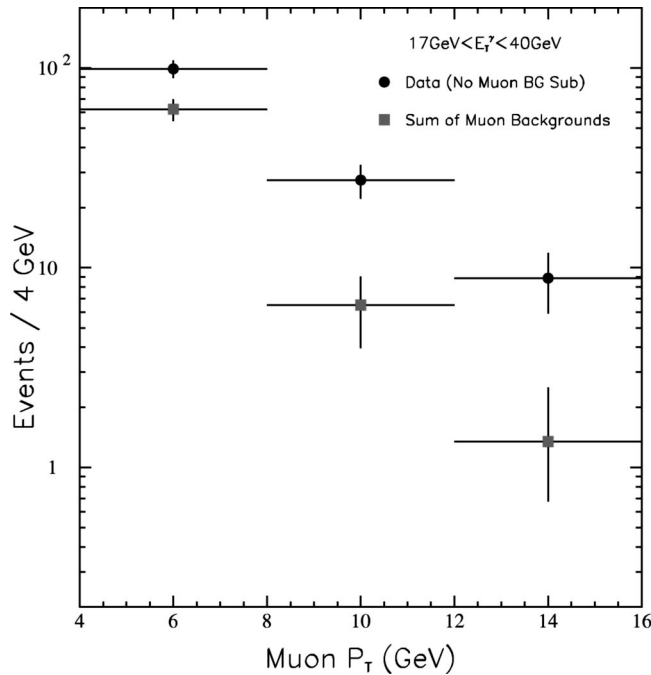
FIG. 3. The muon p_t distribution in direct photon events is shown. The sum of all muon backgrounds is also shown.

FIG. 4. The probability from PYTHIA for a charm quark to give a >4 GeV muon is shown as a function of the charm quark P_T.

the data by studying pions from reconstructed K_s decays. This estimate agrees well with the simulation result, but is statistically weaker, thus the simulation result will be used.

Subtracting the estimated background leaves 72 ± 20 (statistical) direct photon+muon signal events. The photon-muon cross section is derived from the 72 photon-muon events by dividing by the luminosity, 13.2 pb^{-1}, and the efficiencies for detecting the photon within $|\eta_\gamma| < 0.9$ and the muon within $|\eta_\mu| < 1.0$. These efficiencies are measured by a combination of simulation and data studies, which are described in the earlier references. The photon efficiency is $\approx 33\%$ with a small photon P_T dependence, while the muon efficiency is $\approx 57\%$ and depends slightly on the specific muon detector. The resulting photon-muon cross section is $\sigma^{data} = 29$ pb ± 8 pb (statistical).

There are four significant systematic uncertainties on direct photon+muon cross section: (1) 10% from the muon background subtraction, which mostly comes from the uncertainties in the estimated pion and kaon particle fractions, (2) 9% from the photon background subtraction uncertainty, (3) 5% from the uncertainty in the photon and muon cut efficiencies, and (4) 3.6% from the uncertainty in the CDF luminosity measurement. These added in quadrature are a 4 pb uncertainty, much smaller than the statistical uncertainty in the measurement. The measured photon-muon cross section including systematic uncertainties is therefore $\sigma^{data} = 29$ pb ± 9 pb (statistical+systematic).

The photon-muon cross section will be compared to two different QCD calculations of photon-muon production. The first QCD calculation is the PYTHIA [7] Monte Carlo program which only has the leading-order contributions to the photon +heavy quark cross section, but has the full parton shower
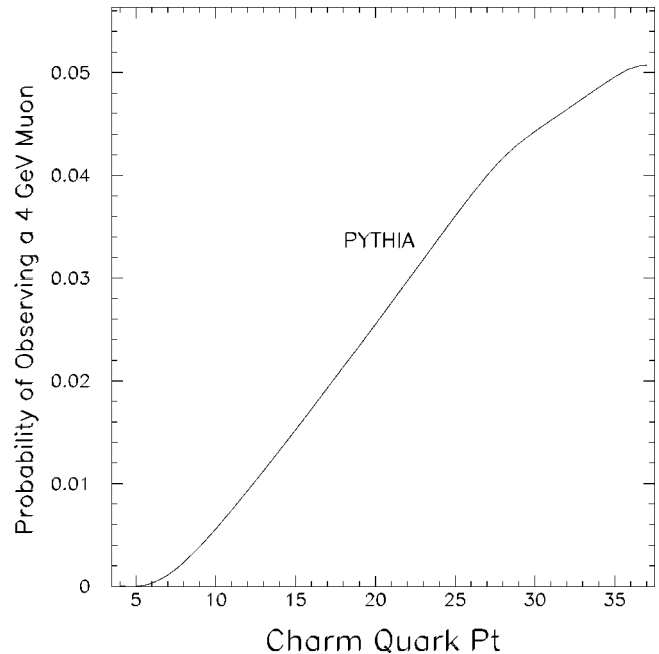
and fragmentation effects, and includes the photon+bottom process (about 25% of the total cross section). The second QCD calculation is the NLO QCD photon+charm calculation detailed in Ref. [1]. This has additional processes not present at leading order, of which Fig. 1b is the largest contribution. But with only the charm quark in the final state in the NLO QCD calculation, we need to convolute it with the effects of charm quark fragmentation. We will use the Peterson fragmentation model in PYTHIA to do this. An example of the resulting probability of observing a 4 GeV muon from this model is shown in Fig. 4 as a function of charm quark P_T. This curve includes the 10% branching ratio and the charm fragmentation effects. This calculation uses the massless quark approximation, which is adequate for photon +charm since the scale of the process is well above the charm mass, but cannot be applied to the photon+bottom process.

The resulting QCD cross sections for photon+muon production are tabulated in Table I, along with the measured value. While both models are consistent with the data within two standard deviations, the NLO QCD predictions are significantly larger than PYTHIA, and closer to the measured value. The ratio of the measurement to PYTHIA is very similar to that observed in our previous publication using reconstructed D^*s to tag the charm quark [2]. A number of varia-

TABLE I. Comparison of the measured photon+muon cross section with the QCD models.

Photon+muon data	PYTHIA (CTEQ4L, $\mu = P_T/2$)	NLO QCD (CTEQ4M, $\mu = P_T/2$)
29 ± 9 pb	13 pb	21 pb

tions of the NLO QCD calculation were investigated, such as renormalization scale, parton distributions, Peterson parameters. The largest variations came from the Peterson parameters: a ± 0.02 change in the fragmentation parameter caused the NLO QCD cross section to change by $\pm 6\%$.

In summary, the first measurement of direct photon plus associated muon production in hadronic interactions has been presented. Comparisons with NLO QCD photon + heavy quark production have also been presented, and are consistent with the measurement.

---

[1] B. Bailey, E. L. Berger, and L. E. Gordon, Phys. Rev. D **54**, 1896 (1996), and references therein.

[2] CDF Collaboration, F. Abe *et al.*, Phys. Rev. Lett. **77**, 5005 (1996).

[3] CDF Collaboration, F. Abe *et al.*, Nucl. Instrum. Methods Phys. Res. A **271**, 387 (1988), and the references therein. The coordinate system used within the CDF is (θ, ϕ), where θ is the polar angle relative to the proton beam as measured from the event vertex, and ϕ the azimuth. The pseudorapidity is defined as $\eta = -\ln \tan(\theta/2)$.

[4] CDF Collaboration, F. Abe *et al.*, Phys. Rev. Lett. **68**, 2734 (1992); Phys. Rev. D **48**, 2998 (1993).

[5] R. T. Hamilton, Ph.D. thesis, Harvard University, 1996.

[6] CDF Collaboration, F. Abe *et al.*, Phys. Rev. D **50**, 2966 (1994).

[7] T. Sjöstrand, CERN-TH 6488, 1992, and references therein. We used version 5.6 of PYTHIA.